BJP BRITISH JOURNAL OF PHARMACOLOGY

BPS BRITISH PHARMACOLOGICAL SOCIETY

British Journal of Pharmacology (2010), 159, 1693–1703

0007-1188/10
www.brjpharmacol.org

RESEARCH PAPER

Naringin improves bone properties in ovariectomized mice and exerts oestrogen-like activities in rat osteoblast-like (UMR-106) cells

Wai-Yin Pang[1,2], Xin-Lun Wang[3], Sau-Keng Mok[1,2], Wan-Ping Lai[1,2], Hung-Kay Chow[4], Ping-Chung Leung[5], Xin-Sheng Yao[3,6] and Man-Sau Wong[1,2]

[1]*Department of Applied Biology and Chemical Technology, The Hong Kong Polytechnic University, Hung Hom, Kowloon, Hong Kong, China,* [2]*State Key Laboratory of Chinese Medicine and Molecular Pharmacology, Shenzhen, China,* [3]*College of Traditional Chinese Materia Medica, Shenyang Pharmaceutical University, Shenyang, China,* [4]*Department of Health Technology and Informatics, The Hong Kong Polytechnic University, Hung Hom, Kowloon, Hong Kong, China,* [5]*Department of Orthopaedics and Traumatology, The Chinese University of Hong Kong, Hong Kong, China, and* [6]*Institute of Traditional Chinese Medicine & Natural Products, College of Pharmacy, Jinan University, Guangzhou, China*

Background and purpose: Naringin, a flavanone glycoside in citrus fruits, has been recently reported to stimulate bone formation *in vitro* and *in vivo*. The present study was designed to determine if naringin could exert oestrogen-like protective actions in bone.

Experimental approach: Young C57/BL6J mice were ovariectomized (OVX) and treated orally with naringin (0.2 or 0.4 $mg \cdot g^{-1} \cdot day^{-1}$), 17β-oestradiol (2 $\mu g \cdot g^{-1} \cdot day^{-1}$) or its vehicle for 6 weeks. Bone mineral densities (BMD) and polar stress-strain index (SSI) were measured by peripheral quantitative computed tomography. Rat osteoblast-like UMR-106 cells were co-incubated with the oestrogen receptor (ER) antagonist ICI 182780 to determine if the effects of naringin on osteoblastic functions were ER dependent. Functional transactivation of ERα and ERβ as well as ERα phosphorylation by naringin were also studied.

Key results: Naringin at 0.4 $mg \cdot g^{-1} \cdot day^{-1}$ increased BMD at trabecular-rich bone in OVX mice. Naringin (at both doses) significantly increased SSI at distal femur and lumbar spine and increased biomechanical strength (ultimate load and energy for breaking) at tibia diaphysis in OVX mice. The stimulatory effects of naringin on osteoblastic functions could be abolished by co-incubation with ICI 182780 in UMR-106 cells. Naringin failed to stimulate ERα- or ERβ-mediated oestrogen response element-dependent luciferase activity but could significantly induce ERα phosphorylation at serine 118, in UMR-106 cells.

Conclusions and implications: Naringin was effective in protecting against OVX-induced bone loss in mice and its actions might be mediated through ligand-independent activation of ER in osteoblastic cells.

British Journal of Pharmacology (2010) **159,** 1693–1703; doi:10.1111/j.1476-5381.2010.00664.x; published online 23 March 2010

Keywords: naringin; osteoprotegerin; RANKL; oestrogen receptors; BMD

Abbreviations: AF, activation function; ALP, alkaline phosphatase; BMD, bone mineral density; BMP, bone morphogenetic protein; DMEM, Dulbecco's modified Eagle's medium; DPD, deoxypyridinoline; E2, 17β-oestradiol; ECL, enhanced chemiluminescence; ER, oestrogen receptor; ERE, oestrogen response element; ERT, oestrogen replacement therapy; GAPDH, glyceraldehyde-3-phosphate dehydrogenase; MAPK, mitogen-activated protein kinase; MTS, 3-(4,5-dimethylthiazol-2-yl)-5-(3-carboxymethoxyphenyl)-2-(4-sulphophenyl)-2H-tetrazolium; OPG, osteoprotegerin; OVX, ovariectomy; PBS, phosphate-buffered saline; PMS, phenazine methosulphate; PNP, *p*-nitrophenylphosphate; polar-SSI, polar stress-strain index; pQCT, peripheral quantitative computed tomography; RANKL, nuclear factor-κB ligand; RT, reverse transcriptase; sFBS, charcoal-stripped fetal bovine serum

Introduction

Osteoporosis is a condition characterized by low bone mineral density (BMD) and micro-architectural deterioration of bone tissue, resulting in an increased risk of fracture (Lau and Cooper, 1996). Increased risks of morbidity and mortality

Correspondence: Dr Man-Sau Wong, Department of Applied Biology and Chemical Technology, The Hong Kong Polytechnic University, Hung Hom, Kowloon, Hong Kong, China. E-mail: bcmswong@polyu.edu.hk
Received 10 May 2009; revised 18 November 2009; accepted 10 December 2009

were found in osteoporotic patients suffering from hip and vertebral fractures (Gass and Dawson-Hughes, 2006). Oestrogen replacement therapy (ERT), which used to be the major treatment for the prevention and treatment of osteoporosis, was recently found to be associated with an increased risk in developing endometrial and breast cancer in postmenopausal women (Wei *et al.*, 2007). Thus, alternative approaches for the prevention and management of postmenopausal osteoporosis, such as the use of natural food ingredients, are worth exploring.

Naringin is a citrus flavonoid commonly found in the pericarp (albedo, membrane and pith) of citrus fruits (Lu *et al.*, 2006). Because of its high daily consumption from citrus fruit and wide availability from inexpensive raw material, there have been numerous studies of the bioactivities of naringin and its potential for treating of diseases. It appears to be useful for improving cardiovascular health and have potential anticancer effects (So *et al.*, 1996; Kim *et al.*, 2006; Benavente-Garcia and Castillo, 2008). Recently, the health benefits of naringin on bone have also received much attention. Deyhim *et al.* (2006; 2008a,b) demonstrated that grapefruit juice could improve bone quality and bone strength in orchidectomized rats. In addition, naringin was shown to improve bone quality in rats with osteoporosis induced by retinoic acid (Wei *et al.*, 2007) and orchidectomized rat (Mandadi *et al.*, 2008) models, confirming that naringin is the active ingredient that accounts for the bone protective effects of citrus fruit. Moreover, naringin significantly increased proliferation, total protein content and alkaline phosphatase (ALP) activities in rat osteoblastic-like UMR-106 cells (Wong and Rabie, 2006). The stimulatory effects of naringin on bone morphogenetic protein-2 (BMP-2) expression in MC3T3-E1 osteoblastic cells were found to be mediated through the activation of the P13K, Akt, c-Fos/c-Jun and AP-1 pathways (Wu *et al.*, 2008). However, it is unclear whether other molecular pathways are also involved in mediating the actions of naringin in bone cells.

Recent reports indicated that phytoestrogens can attenuate bone loss associated with oestrogen deficiency in both animal and human studies (Dixon, 2004). Phytoestrogens are phytochemicals that possess differential affinity for and transactivation of oestrogen receptor (ER)α or ERβ (Gutendorf and Westendorf, 2001; receptor nomenclature follows Alexander *et al.*, 2009). Upon binding to ERs, oestrogen can activate ER and regulate the transcriptional activity via its activation function (AF)-2 domain. Moreover, ERs can also be activated ligand-independently by phosphorylation at the AF-1 domain (Lees *et al.*, 1989; Tora *et al.*, 1989; Tzukerman *et al.*, 1994). For example, epidermal growth factor was shown to induce ERα phosphorylation at serine 118 via the mitogen-activated protein kinase (MAPK) pathway (Chen *et al.*, 2002).

Naringenin, the aglycone of naringin, is a phytoestrogen that could bind weakly to and transactivate ERα- and ERβ-mediated oestrogen response element (ERE)-dependent transcription in human embryonic 293 kidney cells (Kuiper *et al.*, 1998). In the present study, we hypothesize that naringin can exert positive effects in bone via ER-dependent pathways. The effects of naringin on bone properties in ovariectomized (OVX) C57/BL6J female mice and in UMR-106 osteoblastic-like cell culture were studied. In addition, its abilities to induce functional transactivation of ERα and ERβ as well as ERα phosphorylation were also characterized.

Methods

Animal care and diet

All animal care and experimental protocols were approved by the Animal Ethics Committee of the Hong Kong Polytechnic University. Fifty one-month old female C57/BL6J mice from The Chinese University of Hong Kong were housed in environmentally controlled central animal facilities. The animals were kept in 22°C, light : dark (12 h : 12 h) conditions and fed with a normal calcium level (0.6% Ca) control diet for 2 days before the treatment. The mice were either sham operated or OVX at the age of 1 month. After recovering for 2 weeks, the mice were randomly selected and divided into five groups. One group was sham vehicle (2% ethanol), the others were OVX + vehicle; OVX + 17β-oestradiol (E2; 2 $\mu g \cdot g^{-1} \cdot day^{-1}$) and two groups of OVX + naringin (0.2 and 0.4 $mg \cdot g^{-1} \cdot day^{-1}$). The dosages of naringin were chosen based on a previously reported rat study (Wei *et al.*, 2007). Treatments were given orally to the five groups of animals for 6 weeks. Animals were pair fed with diet containing 0.6% Ca and 0.65% P (TD 98005, Teklad, Madison, WI, USA) and were allowed free access to water throughout the course of the studies as previously described (Xie *et al.*, 2005). One day before killing, the mice were placed in metabolic cages. Their urine was collected and centrifuged (1503× *g* for 20 min). The urine samples were then stored at –20°C until use. At the end of treatment, the mice were anesthetized with ketamine (75 $mg \cdot kg^{-1}$; Alfamedic Ltd., Woerden, the Netherlands). Blood samples were taken from the inferior vena cava, followed by the collection of uteri and bone specimens, namely femur, tibia and lumbar spine. The mice serum was stored at –80°C; the left femur, tibia and lumbar spine were stored at –20°C until analysis.

Biochemical assays of serum and urine samples

Calcium and phosphorus concentrations of serum and urine were studied by the *o*-cresolphthalein complexing colour development method and the *p*-methylaminophenol method, respectively, using commercial kits (Wako Pure Chemical Industries Ltd., Osaka, Japan). Urinary excretion of deoxypyridinoline (DPD), a collagen degradation product that reflects bone resorption rate, was measured using Quidel Metra® DPD EIA kit with a microplate reader. Urinary creatinine (Cr) was used as internal control and was assessed with the Jaffe method using a commercial kit (Wako Pure Chemical Industries Ltd.). Urinary calcium, phosphorus and DPD levels were expressed as its excretion per unit of Cr (Ca/Cr, P/Cr and DPD/Cr).

Assessment of bone properties by peripheral quantitative computed tomography (pQCT)

Trabecular and cortical bone densities of left femur, tibia and lumbar spine region L1 were measured using a StraTec XCT2000 machine (Norland Stratec Medizintechnik, GmbH, Birkenfeld, Germany). Mid-shaft and distal regions of femur

and tibia were scanned. The distal/proximal site was defined as 2.5 mm away from femur/tibia head. The mid-shaft was the middle region of each long bone. All scans were performed using the protocol designed for studying isolated small bones (Gasser, 2002). Total BMD, trabecular BMD, total cross-sectional area, trabecular cross-sectional area and stress-strain index (SSI) in the distal/proximal site were determined.

Biomechanical measures of tibia mid-diaphysis

After bone scanning, the left tibia was preserved immediately in phosphate-buffered saline (PBS) and stored at 4°C until the performance of a 3-point bending test (Zhang *et al.*, 2008). Mechanical strength on mid-shaft tibia was measured using specified 3-point bending machine (Hounsfield Test equipment, UK). The anterior side, which was the point receiving compression, was placed upwards. Known loads were applied on the mid-shaft tibia until fracture occurred. All the specimens were pressed at a displacement of 5 $mm \cdot min^{-1}$, and a load–deformation curve was plotted simultaneously. Structural properties (including ultimate load and stiffness) were determined from the load–deformation curve. The material properties were determined based on the calculations of the curve with beam bending theory such as flexural modulus.

Culture of rat osteoblastic UMR-106 cells

UMR-106 cells (ATCC no. CRL-1661) were cultured in Dulbecco's modified Eagle's medium (DMEM) supplemented with 10% fetal bovine serum (FBS), penicillin 100 $U \cdot mL^{-1}$ and streptomycin 100 $\mu g \cdot mL^{-1}$ at 37°C in a humidified atmosphere of 95% air and 5% CO_2 as previously described (Xie *et al.*, 2005). At 80–90% confluence, cells were seeded in 96-well, 24-well or 6-well plates at a density of 3.5×10^3, 2.5×10^4 or 5×10^4 cells per well, respectively, for different assays. After 48 h, the medium was changed to phenol-red free DMEM supplemented with 1% dextran–charcoal-stripped serum (sFBS) for 24 h. The cells were then treated with naringin (0.1 nM to 10 μM), E2 (10 nM) or vehicle in the presence or absence of ICI 182780 (1 μM) for 48 h before treatment.

Cell proliferation assay and ALP activity

The CellTiter 96® AQ_{ueous} non-radioactive cell proliferation assay (Promega Corporation, Madison, MI, USA, #G3580) comprises a novel tetrazolium compound 3-(4,5-dimethylthiazol-2-yl)-5-(3-carboxymethoxyphenyl)-2-(4-sulphophenyl)-2H-tetrazolium (MTS) and an electron coupling reagent (phenazine methosulphate; PMS). After treating with naringin (0.1 nM to 10 μM), E2 (10 nM) or vehicle in the presence or absence of ICI 182780 for 48 h, the medium was discarded and replaced by 0.2 $mg \cdot mL^{-1}$ MTS with 50 $\mu L \cdot mL^{-1}$ PMS. The absorbance was then observed in a microplate reader at 490 nm after 2 h of incubation. ALP activity was measured directly on the monolayer of cell cultures. After medium removal, the cells were washed twice with PBS and dried for 5 min. The enzyme activities of the cell were inactivated by a freeze-and-thaw cycle. Also, 100 μL per well of PBS containing 10 mM *p*-nitrophenylphosphate (PNP) was added and shaken for 30 min at 37°C. The absorbance of colour change was measured at 405 nm in a microplate reader. To normalize the result, Bradford protein assay was carried out and ALP activity was expressed in as $units \cdot L^{-1} \cdot (\mu g\ protein)^{-1}$.

Real-time quantitative reverse transcriptase-polymerase chain reaction (RT-PCR) analysis

Total RNA was extracted from the treated cells using TRIzol® reagent according to the manufacturer's instructions (Invitrogen, Rockville, MD, USA). The concentration and purity of the RNA were determined by measuring the absorbance at 260 and 280 nm (Lau *et al.*, 2008). Two micrograms of total RNA was reversely transcribed to cDNA using a high-capacity cDNA reverse transcription kit purchased from Applied Biosystems (Foster, CA, USA). The mRNA of receptor activator of nuclear factor-κB ligand (RANKL) and osteoprotegerin (OPG) was determined by quantitative real-time PCR using 7900HT Fast Real-time PCR system (Applied Biosystems). The cDNA was amplified with 600 nM of gene specific primers: for OPG, sense: GACGAGATTGAGAGAACGAG, antisense: GGTGCTTGACTTTCTAGGTG; for RANKL, sense: TCAGGAGTTCCAGCTATGAT, antisense: CCATCAGCTGAAGATAGTCC; for glyceraldehyde-3-phosphate dehydrogenase (GAPDH), sense: TACATTTTGCTGATGACTGG, antisense: TGAATGGTAGGAGCTTGACT. The PCR program was carried out as follows: denaturation 95°C for 20 s, amplification for 40 cycles (95°C for 1 s; 53/60°C for 20 s and 72°C for 20 s). Post-PCR dissociation curves were used to confirm the specificity of single-target amplification. The amount of cDNA of each amplification was calculated by using a standard curve which was generated from the negative control group (Lau *et al.*, 2008). Expression levels of RANKL and OPG were normalized to the expression of GAPDH, a housekeeping gene. Modulation of osteoclastogenesis was presented as the ratio between the level of OPG and RANKL mRNA expression.

Transient transfection and ER-mediated luciferase activity assay

Cells were seeded in a 12-well plate at a density of 5×10^4 cells per well and cultured in phenol red-free DMEM supplemented with 1% charcoal-stripped serum for 48 h. The cells were transfected by Lipofectamine™ 2000 reagent as previously described (Lau *et al.*, 2008). ER-α, ER-β and ERE-containing luciferase reporter plasmid vERETkluc were kindly provided by Dr Vincent Giguere (McGill University, Montreal, Quebec, Canada). Also, 0.4 μg per well ER-α or ER-β plasmid, 0.4 μg per well vERETkluc, together with 0.1 μg per well internal control reporter plasmid pRL-TK, a Renilla luciferase control vector, were co-transfected into the cells in duplicate. After 6 h of transfection, the cells were treated with vehicle, E2 (10 nM) or naringin (10 nM and 0.1 μM) for 24 h. After treatment, the cells were lysed with passive lysis buffer and luciferase activity was measured using Dual Luciferase Reporter Assay System (Promega Corporation) and the signal was detected by TD-20/20 Luminometer (Turner Design, Sunnyvale, CA, USA). The oestrogen promoter activity was expressed as *Firefly* luciferase values normalized by pRL-TK Renilla luciferase values.

Immunoblotting
Treated cells were harvested and lysed with passive lysis buffer (Promega) as previously described (Lau *et al*., 2008). Protein concentrations were determined using the Bradford assay. Equal amounts of proteins were separated by sodium dodecyl sulphate–polyacrylamide gel electrophoresis on a 10% reducing gel at a constant voltage (200 V) for about an hour, and transblotted onto polyvinylidene fluoride fluoropolymer membranes (Immobilin-P, Millipore Corp., Billerica, MA, USA). Immunodetection was performed after blocking the non-specific binding sites on the membrane with 5% skimmed milk. The blots were probed with monoclonal rabbit anti-human phospho-ER-α (pERα; phosphorylated at serine 118) (1:2000) or anti-human ER-α (1:3000), and followed by incubation with goat anti-rabbit conjugated with horseradish peroxidase (1:2000). The antigen-antibody complexes were then detected with enhanced chemiluminescence (ECL) reagent and visualized by the Lumi-Imager using Lumi-Analyst version 3.10 software (Roche, Mannheim, Germany)

Statistical analysis
The *in vivo* data were analysed by one-way ANOVA followed by Tukey's post test and the *in vitro* data were analysed by the unpaired Student's *t*-test between control group and each treatment group using Graphpad PRISM® software package. Results were expressed as means ± SEM. *P*-values <0.05 were considered as significant.

Materials
All reagents for cell culture, RT-PCR and plasmid transient transfection kit were purchased from Life Technologies Inc. (Carlsbad, CA, USA) unless otherwise indicated. pRL-TK plasmid and Dual Luciferase Reporter Assay System were from Promega. Naringin and E2 were purchased from Sigma-Aldrich (St. Louis, MO, USA). ICI 182780 was purchased from Tocris Cookson Ltd. (Avonmouth, Bristol, UK). Antibodies directed against ER and horseradish peroxidase-conjugated anti-rabbit IgG antibody were from Santa Cruz Biotechnology (CA, USA). Antibody against pERα (serine 118) was purchased from Upstate (Millipore). ECL detection reagents were obtained from Pierce (Rockford, IL, USA). Primers were obtained from Tech Dragon Ltd (Hong Kong, China).

Results

In vivo *studies*
Body and uterine weight and serum and urinary biochemical markers. The effects of naringin on weight gain, serum and urinary biochemical markers are summarized in Table 1. Weight gain decreased significantly in the OVX mice treated with E2 or with two doses of naringin ($P < 0.05$ vs. OVX + veh). Treatment with E2, but not with naringin, increased uterine weight significantly in OVX mice ($P < 0.05$). The results suggested that naringin did not mimic oestrogen to exert uterotrophic effects in mice. E2 altered serum P, but not serum Ca, in the OVX mice ($P < 0.05$ vs. OVX + veh). The OVX mice treated with naringin (0.2 $mg \cdot g^{-1} \cdot day^{-1}$ or 0.4 $mg \cdot g^{-1} \cdot day^{-1}$) did not have altered serum P or Ca.

By itself, OVX increased urinary Ca excretion in the mice ($P < 0.001$ vs. Sham + veh). The higher dose of naringin (0.4 $mg \cdot g^{-1} \cdot day^{-1}$) or E2 suppressed OVX-induced increase in urinary Ca excretion by 39 and 44% in the OVX mice ($P < 0.05$ vs. OVX + veh) respectively. The OVX mice treated with the lower dose of naringin had decreased urinary Ca levels, but these effects did not reach statistical significance.

Urinary DPD level is a biochemical marker for assessing bone resorption (Huber *et al*., 2003). Table 1 shows that OVX led to a significant increase in urinary DPD level ($P < 0.05$ vs. Sham + veh), while treatment of the OVX mice with E2 suppressed urinary DPD level by 48% ($P < 0.01$ vs. OVX + veh). However, naringin failed to alter urinary DPD level in the OVX mice.

BMD and cross-sectional area. Table 2 summarizes the effects of different treatments on BMD in the distal femur, proximal tibia and lumbar spine region L1 in the sham and OVX mice. OVX significantly decreased the total and trabecular BMD in the distal femur and proximal tibia as well as decreased the total BMD in the lumbar spine in the mice ($P < 0.001$ vs. Sham). Treatment of the OVX mice with E2 significantly restored the total and trabecular BMD at all sites measured ($P < 0.001$ vs. OVX + veh). Treatment of the OVX mice with the lower dose of naringin (0.2 $mg \cdot g^{-1} \cdot day^{-1}$) significantly increased the total BMD of the distal femur and the trabecular BMD of the proximal tibia by 12 and 26% respectively ($P < 0.05$ vs. OVX + veh). A higher dose of naringin (0.4 $mg \cdot g^{-1} \cdot day^{-1}$) significantly increased the total BMD at all

Table 1 Effects of naringin on body and uterine weight and serum and urinary biochemical markers in sham and OVX mice

	Body weight (% change)	*Uteri index ($mg \cdot g^{-1}$)*	*Serum Ca ($mg \cdot L^{-1}$)*	*Serum P ($mg \cdot L^{-1}$)*	*Urinary Ca/Cr ($mg \cdot mg^{-1}$)*	*Urinary P/Cr ($mg \cdot mg^{-1}$)*	*Urinary DPD/Cr ($mg \cdot mg^{-1}$)*
OVX + Veh	3.01 ± 0.096	0.28 ± 0.04	66.9 ± 3.2	88.6 ± 4.8	0.89 ± 0.09	5.65 ± 0.31	38.93 ± 4.95
E2	2.41 ± 0.082*†	2.69 ± 0.18*	64.8 ± 2.4	107.8 ± 6.1*	0.50 ± 0.05*	4.34 ± 0.40	20.21 ± 1.56*
NAR 0.2	2.39 ± 0.085*†	0.28 ± 0.06	69.3 ± 2.5	90.7 ± 3.5	0.70 ± 0.05	5.41 ± 0.49	33.41 ± 2.77
NAR 0.4	2.10 ± 0.069*†	0.32 ± 0.04	72.0 ± 2.1	91.4 ± 2.0	0.55 ± 0.05*	4.52 ± 0.31	34.75 ± 2.76
Sham + Veh	3.22 ± 0.096	2.31 ± 0.32*	70.8 ± 2.2	103.6 ± 4.6	0.55 ± 0.05*	6.37 ± 0.61	25.50 ± 2.61*

Sham and OVX mice were subjected to the following treatments for 6 weeks: Sham + Veh, sham-operated vehicle-treated; OVX + Veh, OVX, vehicle-treated; E2, 17β-oestradiol (2 $\mu g \cdot g^{-1} \cdot day^{-1}$); NAR 0.2, naringin (0.2 $mg \cdot g^{-1} \cdot day^{-1}$); NAR 0.4, naringin (0.4 $mg \cdot g^{-1} \cdot day^{-1}$). Results were analysed by one-way ANOVA and expressed as mean ± SEM ($n = 8$).
*$P < 0.05$ versus OVX + Veh.
†$P < 0.05$ versus Sham + Veh.
DPD, deoxypyridinoline.

Table 2 Effects of naringin on BMD and cross-sectional area of the distal femur, proximal tibia and lumbar spine region L1 in Sham and OVX mice

		OVX + Veh	*E2*	*NAR 0.2*	*NAR 0.4*	*Sham + Veh*
Total BMD (mg·ccm^{-1})	Distal femur	335.2 ± 6.5^{a}	453.4 ± 8.5^{c}	375.0 ± 3.2^{b}	386.8 ± 2.4^{b}	394.3 ± 7.2^{b}
	Proximal tibia	240.9 ± 5.9^{a}	325.5 ± 12.7^{c}	270.5 ± 5.1^{a}	286.4 ± 10.4^{b}	283.7 ± 9.8^{b}
	Lumbar spine L1	215.0 ± 6.4^{a}	259.1 ± 7.4^{c}	232.3 ± 3.1^{a,b}	248.9 ± 4.1^{b}	236.9 ± 2.0^{b}
Tra. BMD (mg·ccm^{-1})	Distal femur	334.5 ± 9.9^{a}	463.8 ± 13.7^{c}	360.0 ± 7.0^{a}	392.5 ± 7.2^{b}	404.1 ± 6.2^{b}
	Proximal tibia	237.8 ± 8.1^{a}	333.6 ± 19.8^{b}	300.8 ± 9.2^{b}	285.7 ± 9.7^{a}	286.7 ± 8.8^{a}
	Lumbar spine L1	N.D.				
Total cross-sectional area (mm^2)	Distal femur	3.35 ± 0.17^{a}	4.04 ± 0.12^{a}	3.99 ± 0.17^{a}	4.03 ± 0.22^{a}	4.06 ± 0.20^{a}
	Proximal tibia	2.79 ± 0.49^{a}	3.75 ± 0.58^{a}	4.44 ± 0.47^{a}	4.56 ± 0.16^{a}	4.13 ± 0.58^{a}
	Lumbar spine L1	2.15 ± 0.34^{a}	4.72 ± 0.48^{c}	3.40 ± 0.32^{a,b}	3.57 ± 0.15^{b}	3.14 ± 0.29^{b}
Trabecular cross-sectional area (mm^2)	Distal femur	1.30 ± 0.16^{a}	1.80 ± 0.07^{b}	1.69 ± 0.09^{a}	1.89 ± 0.10^{b}	1.83 ± 0.11^{b}
	Proximal tibia	1.03 ± 0.13^{a}	1.63 ± 0.25^{a}	1.63 ± 0.22^{a}	1.89 ± 0.09^{b}	1.94 ± 0.22^{b}
	Lumbar spine L1	N.D.				

Sham (Sham + Veh) and OVX mice were subjected to treatments with 17β-Oestradiol (E2), two doses of naringin (NAR 0.2 and NAR 0.4) or its vehicle (OVX + Veh) for 6 weeks. Tibia was subjected to pQCT measurement. N.D. stands for not determined. Data are shown as mean ± SEM and results were analysed by one-way ANOVA ($n = 7$).
[a–c]Means with different superscripts within a row are significantly different ($P < 0.05$). BMD, bone mineral density.

Table 3 Effects of naringin on stress-strain index (SSI) at femur, tibia and lumbar spine in Sham and OVX mice

	OVX + Veh	*E2*	*NAR 0.2*	*NAR 0.4*	*Sham + Veh*
Femur					
Proximal	0.467 ± 0.032^{a}	0.676 ± 0.053^{b}	0.489 ± 0.022	0.572 ± 0.017	0.660 ± 0.025^{b}
Mid-shaft	0.196 ± 0.004^{a}	0.279 ± 0.019^{b}	0.201 ± 0.004	0.212 ± 0.010	0.229 ± 0.010^{b}
Distal	0.380 ± 0.049^{a}	0.714 ± 0.055^{b}	0.613 ± 0.048^{b}	0.714 ± 0.055^{b}	0.738 ± 0.032^{b}
Tibia					
Proximal	0.200 ± 0.037	0.486 ± 0.120	0.325 ± 0.073	0.300 ± 0.038	0.400 ± 0.065
Mid-shaft	0.121 ± 0.010	0.153 ± 0.010	0.136 ± 0.009	0.154 ± 0.010	0.143 ± 0.014
Lumbar spine	0.400 ± 0.053^{a}	0.888 ± 0.089^{b}	0.588 ± 0.035^{b}	0.613 ± 0.044^{b}	0.563 ± 0.042

Sham (Sham + Veh) and OVX mice were subjected to treatment with 17β-oestradiol (E2), two doses of naringin (NAR 0.2 and NAR 0.4) or its vehicle (OVX + Veh) for 6 weeks. Tibia was subjected to pQCT measurement and SSI was calculated by an in-house programme. Data were shown as mean ± SEM and results were analysed by one-way ANOVA ($n = 7$).
[a,b]Means with different superscripts within a row are significantly different ($P < 0.05$).

three sites by 15–19% as well as the trabecular BMD of the distal femur by 17% in the OVX mice ($P < 0.01$ vs. OVX + veh).

OVX alone did not alter the total cross-sectional area but decreased the trabecular cross-sectional areas of the distal femur and the proximal tibia in the mice ($P < 0.05$ vs. sham + veh). Treatment of the OVX mice with E2 significantly increased the trabecular cross-sectional areas of the distal femur by 38% ($P < 0.05$, vs. OVX + veh). Similarly, treatment of the OVX mice with a high dose of naringin (0.4 mg·g^{-1}·day^{-1}) increased the trabecular cross-sectional area of both distal femur and proximal tibia by 45 and 83% ($P < 0.05$, vs. OVX + veh) respectively. In addition, the total cross-sectional area of lumbar spine L1 in mice was reduced by OVX ($P < 0.05$, vs. sham + veh) and increased by E2 (120%) and a high dose of naringin (66%) (0.4 mg·g^{-1}·day^{-1}) in the OVX mice ($P < 0.05$, vs. OVX + veh).

Simulated bone strength (expressed as SSI). SSI is a parameter derived from pQCT scanning for the assessment of torsional bone strength (Deng and Liu, 2005). As shown in Table 3, OVX significantly decreased SSI at the proximal, mid-diaphysis and distal regions of femur in mice ($P < 0.05$ vs. Sham + veh). Treatment of the OVX mice with E2 significantly restored OVX-induced loss of SSI in the OVX mice at all three regions of femur and increased SSI of the lumbar spine in the OVX mice ($P < 0.01$ vs. OVX + veh). Similarly, treatment of the OVX mice with naringin (0.2 and 0.4 mg·g^{-1}·day^{-1}) significantly increased SSI at the distal femur by 61 and 88% and the lumbar spine region L1 by 47 and 53% ($P < 0.05$ vs. OVX + veh) respectively. However, SSI of the proximal tibia and tibial mid-shaft was not significantly altered by OVX or the treatment with E2 and naringin in the OVX mice.

Biomechanical measures of tibia mid-diaphysis. Biomechanical strengths of the cortical bone in mice tibia were measured by using the 3-point bending test (Zhang *et al.*, 2008). As shown in Table 4, OVX reduced bone strength at tibia diaphysis in mice by decreasing ultimate load and energy for breaking ($P < 0.05$ vs. Sham + veh). Treatment of the OVX mice with E2 significantly increased the ultimate load ($P < 0.001$) as well as breaking force ($P < 0.01$) of tibia diaphysis by 40 and 44% (vs. OVX + veh) respectively. Similarly, 0.2 mg·g^{-1}·day^{-1} naringin significantly increased the ultimate load (by 29%), breaking force (by 22%) and energy for breaking (by 149%) of tibia

Table 4 Effects of naringin on biomechanical bone strengths at tibia diaphysis in Sham and OVX mice

	Ultimate load (N)	*Breaking force (N)*	*Energy for breaking (× 10^{-3} J)*	*Stiffness (N·mm^{-1})*	*Flexural modulus (Mpa)*
OVX + Veh	11.73 ± 0.34	11.36 ± 0.26	4.69 ± 0.59	14.89 ± 1.71	1.31 ± 0.11
E2	16.46 ± 0.76***	16.37 ± 0.66**	6.93 ± 0.51	18.83 ± 1.53	1.84 ± 0.17
NAR 0.2	15.19 ± 0.57**	13.93 ± 0.50*	11.68 ± 2.1**	18.87 ± 2.39	1.79 ± 0.13
NAR 0.4	15.61 ± 0.39***	13.89 ± 0.73	8.70 ± 0.74**	20.15 ± 2.58	2.02 ± 0.24
Sham + Veh	14.71 ± 0.69*	12.45 ± 0.84	8.63 ± 1.18*	23.28 ± 4.90	1.74 ± 0.23

Sham (Sham + Veh) and OVX mice were subjected to treatment with 17β-oestradiol (E2), two doses of naringin (NAR 0.2 and NAR 0.4) or its vehicle (OVX + Veh) for 6 weeks. Tibia was subjected to the three-point bending test and the parameters were calculated by an in-house program. Data were shown as mean ± SEM and the results were analysed by one-way ANOVA ($n = 7$).
*$P < 0.05$; **$P < 0.01$; ***$P < 0.001$ versus OVX + Veh.

diaphysis in the OVX mice ($P < 0.01$ vs. OVX + veh). 0.4 $mg \cdot g^{-1} \cdot day^{-1}$ of naringin significantly increased the ultimate load (by 33%) and energy for breaking (by 85%) of tibia diaphysis in the OVX mice ($P < 0.01$ vs. OVX + veh). However, none of the treatments altered the stiffness and flexural modulus of tibia.

In vitro *studies*

Cell proliferation assay and ALP activity. The dose-dependent effects of naringin on cell proliferation and ALP activity in rat osteoblast-like UMR-106 cells are shown in Figure 1. At 24 h, 10 nM to 1 μM of naringin increased UMR-106 cell proliferation ($P < 0.05$ vs. vehicle). When cells were cultured for 48 h, naringin at all concentrations (0.1 nM to 10 μM) increased osteoblastic cell proliferation. Specifically, 0.1–10 nM naringin effectively increased osteoblastic cell numbers by 30 to 38% ($P < 0.01$ and $P < 0.001$ vs. vehicle). ALP is a common marker for the assessment of osteoblastic cell differentiation. As observed with E2, naringin over a range of concentrations (10 nM–1 μM) significantly increased ALP activity in UMR-106 cells (Figure 1B). Low concentrations of naringin (1 nM) significantly increased osteoblastic cell differentiation by 13% ($P < 0.001$), while 10 nM of E2 increased ALP activity by 15% ($P < 0.001$).

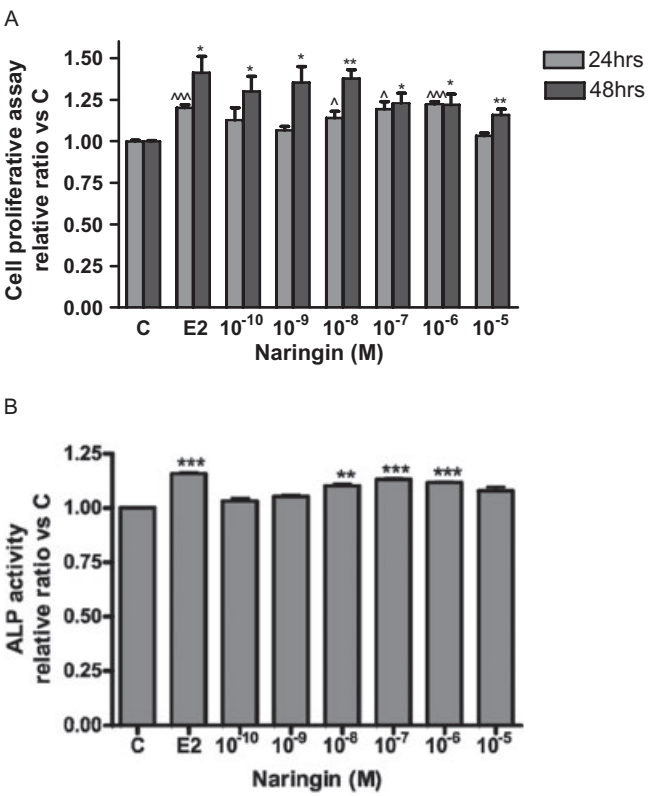

Figure 1 Effects of naringin on cell proliferation and alkaline phosphatase (ALP) activity in UMR-106 cells. (A) UMR-106 cells were treated with vehicle (C), 17β-oestradiol (E2; 10^{-8} M) or 10^{-10}–10^{-5} M of naringin for 24 or 48 h. Cell proliferation rate was assessed by the 3-(4,5-dimethylthiazol-2-yl)-5-(3-carboxymethoxyphenyl)-2-(4-sulphophenyl)-2H-tetrazolium assay. Results were obtained from three independent experiments and were expressed as mean ± SEM. *$P < 0.05$; **$P < 0.01$ versus control (C). ^$P < 0.05$; ^^^$P < 0.001$ versus control. (B) UMR-106 cells were treated with vehicle (C), E2; (10^{-8} M) or 10^{-10}–10^{-5} M of naringin for 24 h. The lysates were used for analysis of ALP activity. Results were obtained from three independent experiments in triplicate and were expressed as mean ± SEM. **$P < 0.01$; ***$P < 0.001$ versus control (C).

Effects of the ER antagonist. To determine if the action of naringin is mediated by the ER, UMR-106 cells treated with naringin were co-treated with a specific ER antagonist, ICI 182780. As shown in Figure 2A, co-treatment of UMR-106 cells with ICI 182780 completely abolished the stimulatory effects of 10 nM of E2 and naringin on cell proliferation. Similarly, co-treatment of UMR-106 cells with ICI 182780 completely abolished the stimulatory effects of 10 nM E2, 10 nM and 100 nM of naringin on ALP activity (Figure 2B).

Expression of mRNA for OPG and receptor activator of RANKL. OPG and RANKL are identified as the dominant and final mediators of osteoclastogenesis (Bord *et al.*, 2003). The secretion of OPG by osteoblastic cells could block the interaction of RANKL with its functional receptor RANK expressed on the osteoclastic cell surface, thereby inhibiting osteoclastogenesis. As shown in Figure 3A, 10 nM of E2 and naringin significantly increased OPG mRNA expression in UMR-106 cells. Their inductive effects on OPG mRNA expression were completely abolished in the presence of the ER antagonist, ICI 182780 ($P < 0.05$). RANKL mRNA expression was not altered by treatment with 10 nM E2 but was down-regulated by treatment with 10 nM naringin in UMR-106 cells (Figure 3B, $P < 0.05$ vs. vehicle). Co-treatment of UMR-106 cells with ICI 182780 suppressed RANKL mRNA expression in both vehicle-treated and E2-treated UMR-106 cells. Co-treatment of UMR-106 cells with naringin and ICI 182780 did not prevent the

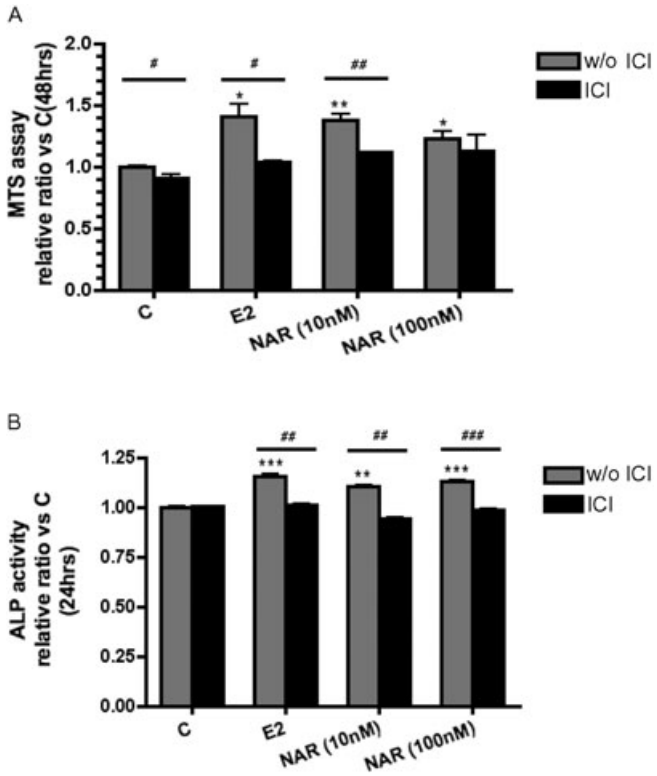

Figure 2 Effects of ICI 182780 on the stimulatory effects of naringin on cell proliferation and differentiation in UMR-106 cells. UMR-106 cells were treated with vehicle (C), 17β-oestradiol (E2; 10^{-8} M) or naringin (10 nM or 100 nM) of naringin in the presence or absence of ICI 182780. (A) Cell proliferation rate was assessed by the 3-(4,5-dimethylthiazol-2-yl)-5-(3-carboxymethoxyphenyl)-2-(4-sulphophenyl)-2H-tetrazolium (MTS) assay. Results were obtained from three independent experiments and were expressed as mean ± SEM. $^{**}P < 0.01$ versus control (C). (B) Cell lysates were used for alkaline phosphatase (ALP) activity measurement. Results were obtained from three independent experiments in triplicate and were expressed as mean ± SEM. $^{*}P < 0.05$; $^{**}P < 0.01$; $^{***}P < 0.001$ versus control; $\#P < 0.05$, $\#\#P < 0.01$; $\#\#\#P < 0.001$ versus ICI-treated cells.

suppressive effects of naringin on RANKL mRNA expression. The ratio of OPG to RANKL mRNA expression was calculated to demonstrate the effects of treatment on osteoclastogenesis. The OPG/RANKL mRNA expression ratio increased in UMR-106 cells in response to treatment with 10 nM E2 and naringin (Figure 3C, $P < 0.05$ vs. its vehicle). Co-treatment of UMR-106 cells with ICI 182780 prevented the inductive effects of E2 and naringin on the OPG/RANKL ratio.

ER-mediated luciferase activity assay. To determine if naringin activates ERE-dependent transcription via the ERα or ERβ, UMR-106 cells treated with either E2 or naringin were co-transfected with ERE-luciferase and ERα or β constructs. Our results indicated that 10 nM E2 activated ERE-dependent luciferase activity via ERα (Figure 4A, $P < 0.001$ vs. its vehicle), as well as ERβ (Figure 4B, $P < 0.01$ vs. its vehicle) in UMR-106 cells. In addition, 100 nM of naringin, but not 10 nM, also induced ERE-dependent luciferase expression via ERα and ERβ in UMR-106 cells (Figure 4A,B, $P < 0.05$ vs. C).

ERα expression and its phosphorylation. To determine if naringin could alter ER expression and induce ligand-independent activation of ER, the levels of ERα and pERα expression were studied. Serine 118 is the phosphorylation site of ER that can be triggered by ligand-independent pathways (Bjornstrom and Sjoberg, 2005). Also, 10 nM of E2 significantly induced pERα protein expression by 50% (Figure 5A,B, $P < 0.05$ vs. its vehicle) and suppressed ERα expression by 23% simultaneously (Figure 5A,C, $P < 0.05$ vs. its vehicle) in UMR-106 cells. Also, 10 nM and 100 nM of naringin significantly induced pERα expression in UMR-106 cells by about 60 and 32% respectively (Figure 5A,B, $P < 0.05$ vs. vehicle). However, naringin did not alter ERα expression in UMR-106 cells at both dosages tested. To assess their overall effects on ER phosphorylation, the relative ratio of pERα versus ERα expression was calculated. As shown in Figure 5D, E2 (10 nM), 10 nM and 100 nM naringin markedly increased pERα/ERα by 85, 21 and 47% respectively ($P < 0.05$ vs. its vehicle).

Discussion

The present study systematically evaluated the osteoprotective effects and mechanism of actions of naringin in OVX mice and in rat osteoblast-like UMR-106 cells. Our results clearly demonstrated that naringin could suppress OVX-induced increase in urinary Ca excretion as well as loss in bone mass and bone strength in OVX mice. In addition, our study showed that naringin mimicked E2 in stimulating cell proliferation, ALP activity and OPG/RANKL mRNA expression via ER in UMR-106 cells, suggesting that it could exert oestrogen-like effects in promoting osteoblastic functions and inhibiting osteoclastogenesis.

Our study demonstrated that treatment of OVX mice with naringin at 0.2 $mg \cdot g^{-1} \cdot day^{-1}$ or 0.4 $mg \cdot g^{-1} \cdot day^{-1}$ for 6 weeks, improved bone quality at the distal femur, proximal tibia and lumbar spine. These results are in agreement with those reported by others regarding the positive effects of naringin on bone quality. Thus, Mandadi *et al.* (2008) reported that treatment with naringin at 200 ppm for 2 months significantly increased plasma IGF-I level, femoral BMD and strength, BMD of the 5th lumbar spine as well as bone Ca content of femur and lumbar spine in young orchidectomized rats. Wei *et al.* (200) reported that treatment with naringin at 20–100 $mg \cdot kg^{-1}$ for 14 days significantly increased femur weight, femur length and diameter of the femoral head, bone Ca and P content as well as BMD of femur, and suppressed serum ALP in young retinoid acid-induced osteoporotic female Sprague Dawley rats. Both these studies suggested that the bone protective action of naringin might not be mediated by the suppression of bone resorption process as urinary DPD levels were not suppressed by naringin in OVX mice or in orchidectomized rats.

Using pQCT analysis, our study demonstrated that naringin at 0.4 $mg \cdot g^{-1} \cdot day^{-1}$ could significantly increase the total BMD of the three trabecular-rich sites, namely the distal femur, proximal tibia and lumbar spine L1, as well as increasing the trabecular cross-sectional area of the distal femur and proximal tibia in OVX mice. In addition, naringin at both 0.2 and 0.4 $mg \cdot g^{-1} \cdot day^{-1}$ increased SSI, the indicator for torsional bone strength (Deng and Liu, 2005), of distal femur as well as lumbar spine L1 in OVX mice. Furthermore, the three-point

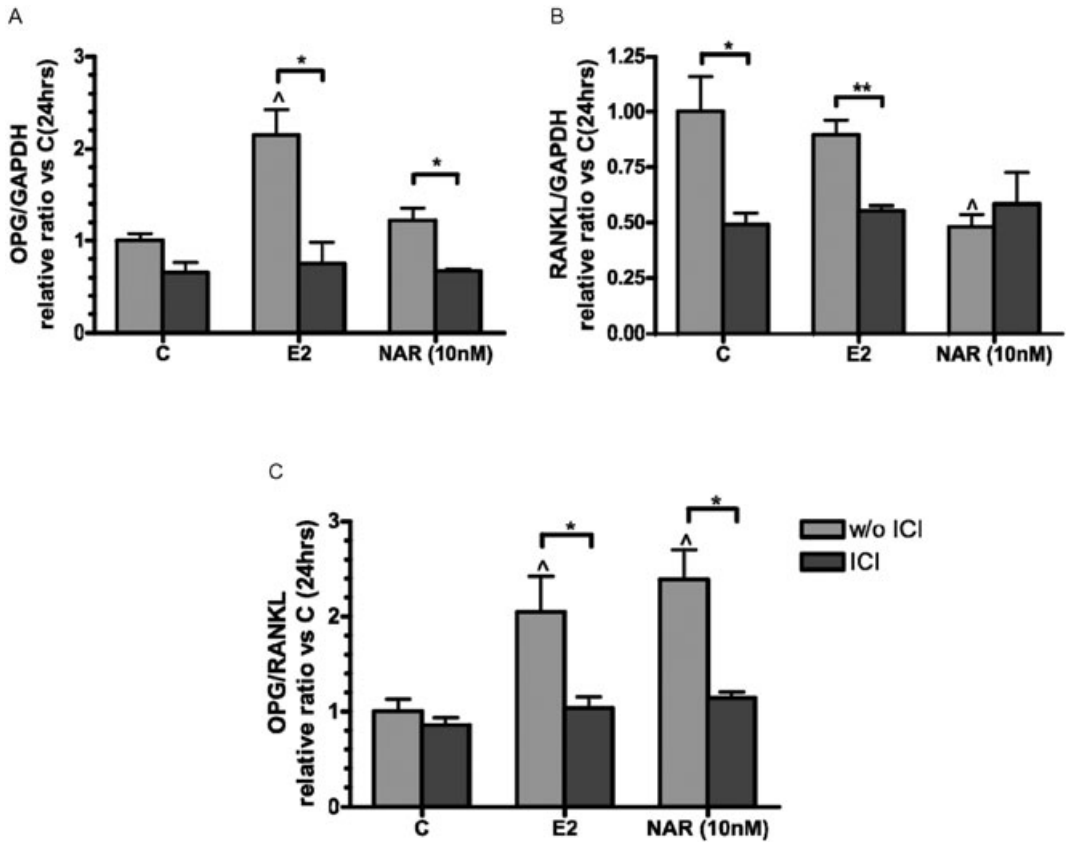

Figure 3 Effects of naringin on osteoprotegerin (OPG) and nuclear factor-κB ligand (RANKL) mRNA expressions in UMR-106 cells. UMR-106 cells were treated with vehicle (C), 17β-oestradiol (E2; 10^{-8} M) or naringin (10 nM) of naringin in the presence or absence of ICI 182780 for 48 h. Total RNA was isolated and real-time-RT-PCR was performed to determine the mRNA expressions of (A) OPG, (B) RANKL and (C) OPG/RANKL, which were normalized to that of glyceraldehyde-3-phosphate dehydrogenase (GAPDH). Results were obtained from two independent experiments in triplicate and expressed as mean ± SEM. ^$P < 0.05$ versus control (C); *$P < 0.05$; **$P < 0.01$ versus ICI-treated cells.

bending experiments demonstrated that naringin could improve the biomechanical strength of cortical bone in OVX mice. The results indicate that naringin could increase total BMD and the biomechanical strength of both trabecular bone-rich as well as cortical bone-rich sites at tibia diaphysis in OVX mice.

Direct effects of naringin on osteoblastic cell proliferation and differentiation in rat osteoblast-like UMR-106 cells (Wong and Rabie, 2006) and murine osteoblastic MC3T3-E1 cells (Wu *et al*., 2008) have been reported by others. The results of the present study confirmed the fact that naringin could stimulate proliferation and ALP activities in UMR-106 cells in a dose-dependent manner. In addition, our results showed that 10 nM naringin could stimulate OPG and suppress RANKL mRNA expression in UMR-106, resulting in an increase in the ratio of OPG : RANKL. These results suggest that naringin might mimic oestrogen to suppress the process of osteoclastogenesis through its direct actions on modulating the expression of OPG and RANKL in osteoblastic cells. Furthermore, it should be noted that the potency of naringin in osteoblastic cell is very high as the results of the present study clearly indicated that naringin can exert stimulatory effects in UMR-106 cells at concentrations as low as 0.1 nM. An earlier study by Erlund *et al*. (2001) reported that the plasma concentration of naringenin reached 6 μM upon ingestion of grapefruit juice (8 mL per kg) in human subjects and that naringin might be absorbed in its intact form (Ishii *et al*., 2000). Thus, the present study showed that such circulating levels of naringin might be able to exert positive effects on bone tissues in individuals who consumed grapefruit product on a regular basis, despite the relatively short half-life of the compounds.

The results of the present study support our hypothesis that naringin can exert positive effects in bone via ER-dependent pathways. We have demonstrated that the stimulatory effects of naringin on cell proliferation, differentiation as well as OPG/RANKL ratio in UMR-106 cells could be abolished by co-treatment with the ER antagonist, ICI 182780. As ICI 182780 is a specific ER antagonist that binds, blocks and increases degradation of ER (Obsborne *et al*., 2004), our results suggest that the ER are involved in mediating the actions of naringin in bone cells. Transfection study indicated that naringin at 100 nM, but not 10 nM, induced ERE-dependent luciferase activities via either ERα or ERβ in UMR-106 cells, suggesting that the action of naringin at high, but not low, concentrations is similar to that of E2.

Naringin is a flavonoid glycoside bearing the rutinose group and is known to be hydrolysed to its aglycone, naringenin only in the distal part of the intestine and the colon by colonic bacteria and subsequently absorbed into the

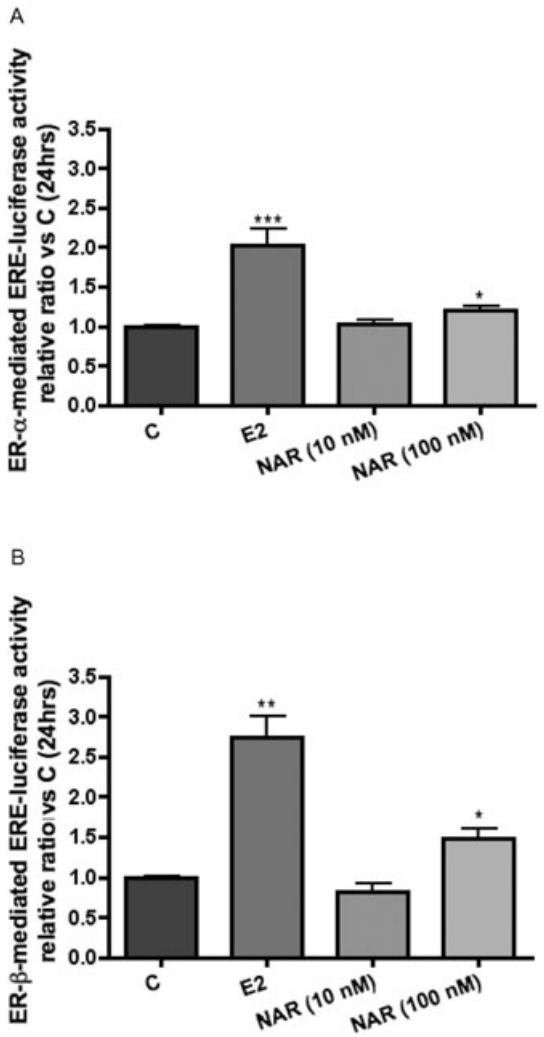

Figure 4 Effects of naringin on ERα- or ERβ-mediated oestrogen response element (ERE)-dependent luciferase activity in UMR-106 cells. Cells were co-transfected with 0.4 μg ERα or ERβ plasmid, 0.4 μg ERE-containing luciferase reporter plasmid and 0.1 μg pRL-TK luciferase internal reporter plasmid using the Lipofectamine 2000 reagent according to the manufacturer's instructions. Transfected cells were treated with vehicle (C), 17β-oestradiol (E2; 10^{-8} M) or naringin [Nar(10 nM) and Nar (100 nM)] for 24 h. Activities of luciferase encoded by experimental and internal control plasmid were measured sequentially with the DLR assay reagents. The ERE *firefly* luciferase activities were normalized for pRL-TK Renilla luciferase values. 100% represents the ERE luciferase activity of the control. Results were obtained from three independent experiments and expressed as mean ± SEM. *$P < 0.05$; **$P < 0.01$; ***$P < 0.001$ versus control (C).

systematic circulation as glucuronides and sulphoglucuronides (Kanaze *et al.*, 2007). It is believed that hydrolysis of the flavanone glycosides to their aglycones might be the rate-limiting step for their absorption (Erlund *et al.*, 2001). Ishii *et al.* (2000) have reported that naringin can also be absorbed in its intact form. Thus, it is unclear if the positive effects of naringin on bone observed in our *in vivo* experiment are due to the effects of naringenin or the combined effects of naringin and naringenin. Nevertheless, our results showed that naringin taken *in vivo* could exert oestrogen-like effects on bone as well as mimicking the suppressive effect of oestrogen on OVX-induced increase in body weight in mice, without inducing any growth of the uterus. These results indicate that naringin can function as a phytoestrogen that exerts selective effects on bone and possibly adipose tissue as well without exerting any unwanted oestrogenic effects in the uterus.

Recent studies also indicated that the ER could be activated in the absence of ligand binding by modulating a variety of signal transduction pathways, such as the MAPK-mediated pathways (Kato *et al.*, 1995; Bunone *et al.*, 1996; Zhang *et al.*, 2008). The activation of unliganded ERα via the MAPK cascade results in three phosphorylations in ERα, at serine 118, serine 104 and serine 167, all within the AF-1 domain of ERα, which in turn modulates the transcriptional activity (Chen *et al.*, 2002). To determine if naringin activates ER ligand-independently, the ratio of phosphorylated ERα (at serine 118) to total ERα expression in UMR-106 cells in response to naringin treatment was studied. ER phosphorylation at serine 118 was chosen as this is a highly conserved residue and represents the major site of phosphorylation in response to E2 (Lannigan, 2003). Our results clearly indicated that naringin could activate ERα phosphorylation in UMR-106 cells, suggesting that naringin could activate ER ligand-independently in osteoblastic cells.

The present study clearly demonstrated that the oestrogen-like actions of naringin *in vivo* are tissue selective and that the ER are involved in mediating the anabolic effects of naringin in osteoblastic cells. The results of the mechanistic studies suggested that the tissue selective effects of naringin might be mediated through its differential abilities to induce phosphorylation of ERα- and ERE-dependent transcriptional activity. Unlike E2, 10 nM of naringin did not activate ERE-dependent transcription via ERα or ERβ in UMR-106 cells, suggesting that the anabolic actions of naringin at 10 nM might not be mediated by ERE-dependent transcriptional activity. In contrast, 10 nM naringin could induce ERα phosphorylation at serine 118 in UMR-106 cells in a ligand-independent manner. Recent studies by Kousteni's group suggested that ligand, which activates kinase-mediated actions of ER, could reverse the loss of bone mass and strength in OVX mice without significant stimulatory effects on reproductive organs (Kousteni *et al.*, 2002), and that kinase-mediated actions of the ER are important for inducing osteoblast differentiation (Kousteni *et al.*, 2007). The fact that naringin could reverse bone loss in OVX mice without any uterotrophic effects suggests that it might induce osteoblast differentiation via kinase-mediated actions of the ER. Further study will be needed to determine if naringin could activate osteoblastic differentiation via kinase-mediated actions of the ER.

Naringin, an active ingredient identified in citrus fruits, is clearly demonstrated to be a phytoestrogen that is effective for protection against bone loss associated with oestrogen deficiency. Its *in vivo* and *in vitro* actions are similar to those of genistein, a well-characterized phytoestrogen in soy, whose *in vivo* tissue selective effects (Zhang *et al.*, 2009) and the high potency (it is active at 10 nM) (Chen and Wong, 2006) were also reported previously. However, the *in vitro* mechanistic study indicated that the mechanism of the oestrogen-like actions of naringin in osteoblastic cells appeared to be different from those reported for genistein, as naringin did not

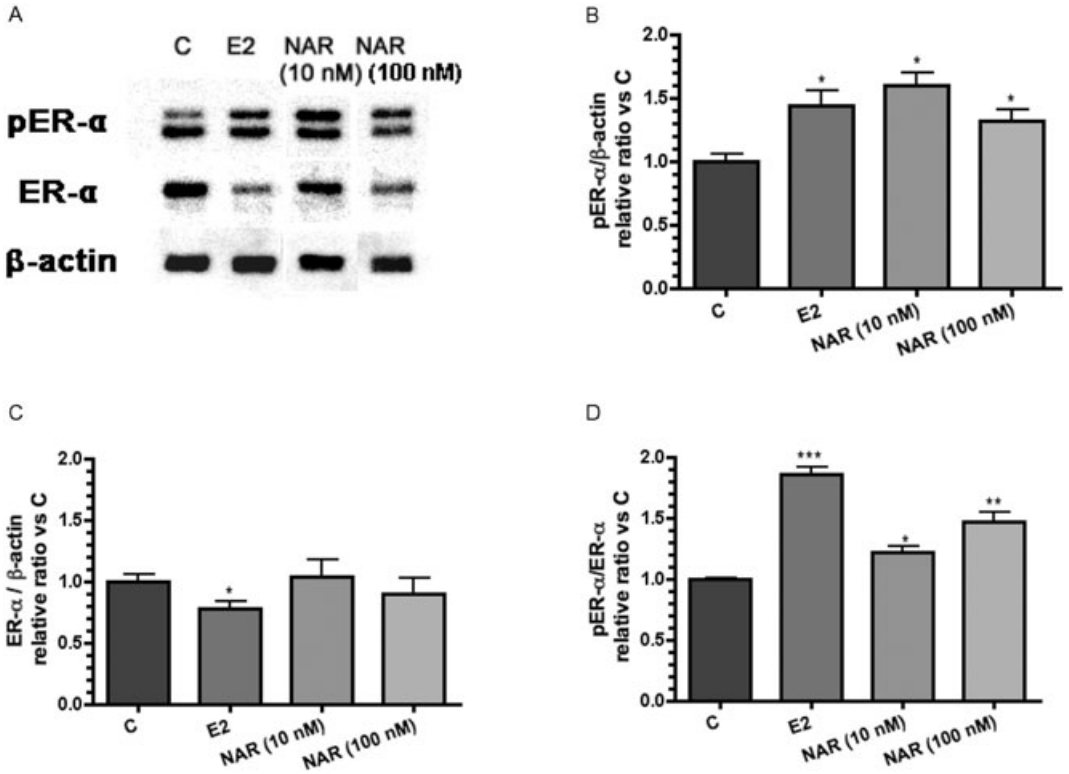

Figure 5 Effects of naringin on phosphorylation of ERα at serine 118, in UMR-106 cells. Cells were treated with vehicle (C), 17β-oestradiol (E2; 10^{-8} M) or naringin [Nar(10 nM) and Nar (100 nM)] for 24 h. Proteins extracted from cell lysates were transblotted onto a membrane and probed with anti-phospho-ERα (at Serine 118) (pERα) and anti-ERα (ERα) primary antibodies followed by the corresponding secondary antibodies. Relative intensity of chemiluminescence was measured and phospho-ERα to ERα ratio was calculated. Protein blots of pERα, ERα and β-actin (A) and graphical presentations of pERα protein expression (B), ERα protein expression (C), ratio of pERα/ERα (D) are shown. Results were obtained from three independent experiments and expressed as mean ± SEM. *$P < 0.05$; **$P < 0.01$; ***$P < 0.001$ versus control (C).

activate ERE-dependent transcription and preferentially activated ER in a ligand-independent manner. In contrast, genistein is known to possess higher binding affinity to ERβ than to ERα and activate ERE-dependent transcription in a ligand dependent manner (Kuiper *et al.*, 1998). Thus, it appears that naringin is a phytoestrogen that exerts a distinct mechanism of action in bone cells. An earlier study showed that hesperidin, another citrus flavonoid, could also inhibit bone loss in OVX mice (Chiba *et al.*, 2003). These earlier results, together with those of the present study, clearly show that citrus flavonoids are useful for improvement of bone properties in animal models of osteoporosis induced by oestrogen deficiency. Further studies will be needed to evaluate the clinical efficacy of citrus flavonoids for treatment of postmenopausal osteoporosis.

Acknowledgements

We thank the State Key Laboratory of Chinese Medicine and Molecular Pharmacology, Shenzhen for its support. This work was supported by the National Science Foundation China/Research Grant Council (N_PolyU536/04), HKSAR and the Niche Area Fund from The Hong Kong Polytechnic University (I-BB8N).

Conflicts of interest

None.

References

Alexander SPH, Mathie A, Peters JA (2009). Guide to receptors and channels (GRAC), 4th edn. *Br J Pharmacol* **158** (Suppl. 1): S1–S254.

Benavente-Garcia O, Castillo J (2008). Update on uses and properties of citrus flavonoids: new findings in anticancer, cardiovascular, and anti-inflammatory activity. *J Agric Food Chem* **56**: 6185–6205.

Bjornstrom L, Sjoberg M (2005). Mechanisms of estrogen receptor signaling: convergence of genomic and nongenomic actions on target genes. *Mol Endocrinol* **19**: 833–842.

Bord S, Ireland DC, Beavan SR, Compston JE (2003). The effects of estrogen on osteoprotegerin, RANKL, and estrogen receptor expression in human osteoblasts. *Bone* **32**: 136–141.

Bunone G, Briand PA, Miksicek RJ, Picard D (1996). Activation of the unliganded estrogen receptor by EGF involves the MAP kinase pathway and direct phosphorylation. *EMBO J* **15**: 2174–2183.

Chen WF, Wong MS (2006). Genistein modulates the effects of parathyroid hormone in human osteoblastic SaOS-2 cells. *Br J Nutr* **95**: 1039–1047.

Chen D, Washbrook E, Sarwar N, Bates GJ, Pace PE, Thirunuvakkarasu V *et al.* (2002). Phosphorylation of human estrogen receptor alpha

at serine 118 by two distinct signal transduction pathways revealed by phosphorylation-specific antisera. *Oncogene* **21**: 4921–4931.

Chiba H, Uehara M, Wu J, Wang X, Masuyama R, Suzuki K *et al*. (2003). Hesperidin, a citrus flavonoid, inhibits bone loss and decreases serum and hepatic lipids in ovariectomized mice. *J Nutr* **133**: 1892–1897.

Deng HW, Liu YZ (2005). *Current Topics in Bone Biology*. World Scientific: Singapore.

Deyhim F, Garica K, Lopez E, Gonzalez J, Ino S, Garcia M *et al*. (2006). Citrus juice modulates bone strength in male senescent rat model of osteoporosis. *Nutrition* **22**: 559–563.

Deyhim F, Mandadi K, Bahram F, Bhimanagoudo SP (2008a). Grapefruit juice modulates bone quality in rats. *J Med Food* **11**: 99–104.

Deyhim R, Mandadi K, Patil BS, Faraji B (2008b). Grapefruit pulp increase antioxidant status and improves bone quality in orchidecotmized rats. *Nutrition* **4**: 1039–1044.

Dixon RA (2004). Phytoestrogens. *Annu Rev Plant Biol* **55**: 225–261.

Erlund I, Meririnne E, Alfthan G, Aro A (2001). Plasma kinetics and urinary excretion of the flavanones naringenin and hesperetin in humans after ingestion of orange juice and grapefruit juice. *J Nutr* **131**: 235–241.

Gass M, Dawson-Hughes B (2006). Preventing osteoporosis-related fractures: an overview. *Am J Med* **119**: S3–S11.

Gasser JA (2002). Bone measurements by peripheral quantitative computed tomography in rodents. *Methods Mol Med* **80**: 323–341.

Gutendorf B, Westendorf J (2001). Comparison of an array of *in vitro* assays for the assessment of the estrogenic potential of natural and synthetic estrogens, phytoestrogens and xenoestrogens. *Toxicology* **166**: 79–89.

Huber F, Traber L, Roth HJ, Heckel V, Schmidt-Gayk H (2003). Markers of bone resorption – measurement in serum, plasma or urine? *Clin Lab* **49**: 203–207.

Ishii K, Furuta T, Kasuya Y (2000). Mass spectrometric identification and high-performance liquid chromatographic determination of a flavonoids glycoside naringin in human urine. *J Agric Food Chem* **48**: 56–59.

Kanaze FI, Bounartzi MI, Georgarakis M, Niopas I (2007). Pharmacokinetics of the citrus flavanone aglycones hesperetin and naringenin after single oral administration in human subjects. *Eur J Clin Nutr* **61**: 472–477.

Kato S, Endoh H, Masuhiro Y, Kitamoto T, Uchiyama S, Sasaki H *et al*. (1995). Activation of the estrogen receptor through phosphorylation by mitogen-activated protein kinase. *Science* **270**: 1491–1494.

Kim SY, Kim HJ, Lee MK, Jeon SM, Do GM, Kwon EY *et al*. (2006). Naringin time-dependently lowers hepatic cholesterol biosynthesis and plasma cholesterol in rats fed high-fat and high-cholesterol diet. *J Med Food* **9**: 582–586.

Kousteni S, Chen JR, Bellido T, Han L, Ali AA, O'Brien CA *et al*. (2002). Reversal of bone loss in mice by nongenotropic signaling of sex steroids. *Science* **298**: 843–846.

Kousteni S, Almeida M, Han L, Bellido T, Jilka RL, Manolagas SC (2007). Induction of osteoblast differentiation by selective activation of kinase-mediated actions of the estrogen receptor. *Mol Cell Biol* **27**: 1516–1530.

Kuiper G, Lemmen JG, Carlsson B, Corton JC, Safe SH, van der Saag PT *et al*. (1998). Interaction of estrogenic chemicals and phytoestrogens with ERβ. *Endocrinology* **139**: 4252–4263.

Lannigan DA (2003). Estrogen receptor phosphorylation. *Steroids* **68**: 1–9.

Lau EM, Cooper C (1996). The epidemiology of osteoporosis. The oriental perspective in a world context. *Clin Orthop Relat Res* **323**: 65–74.

Lau WS, Chan RYK, Guo DA, Wong MS (2008). Ginsenoside Rg1 exerts estrogen-like activities via ligand-independent activation of ERα pathway. *J Steroid Biochem Mol Biol* **108**: 64–71.

Lees JA, Fawell SE, Parker MG (1989). Identification of two transactivation domains in the mouse oestrogen receptor. *Nucleic Acids Res* **17**: 5477–5488.

Lu Y, Zhang C, Bucheli P, Wei D (2006). Citrus flavonoids in fruit and traditional Chinese medicinal food ingredients in China. *Plant Foods Hum Nutr* **61**: 57–65.

Mandadi K, Ramirez M, Jayaprakasha GK, Faraji B, Lihono M, Deyhim F *et al*. (2008). Citrus bioactive compounds improve bone quality and plasma antioxidant activity in orchidectomized rats. *Phytomedicine* **16** (6–7): 513–520.

Obsborne CK, Wakeling A, Nicholson RI (2004). Fulvestrant: an oestrogen receptor antagonist with a novel mechanism of action. *Br J Cancer* **90** (Suppl. 1): S2–S6.

So FV, Guthrie N, Chambers AF, Moussa M, Carroll KK (1996). Inhibition of human breast cancer cell proliferation and delay of mammary tumorigenesis by flavonoids and citrus juices. *Nutr Cancer* **26**: 167–181.

Tora L, White J, Brou C, Tasset D, Webster N, Scheer E *et al*. (1989). The human estrogen receptor has two independent nonacidic transcriptional activation functions. *Cell* **59**: 477–487.

Tzukerman MT, Esty A, Santiso-Mere D, Danielian P, Parker MG, Stein RB *et al*. (1994). Human estrogen receptor transactivational capacity is determined by both cellular and promoter context and mediated by two functionally distinct intramolecular regions. *Mol Endocrinol* **8**: 21–30.

Wei M, Yang Z, Li P, Zhang Y, Sse WC (2007). Anti-osteoporosis activity of naringin in the retinoic acid-induced osteoporosis model. *Am J Chin Med* **35**: 663–667.

Wong RW, Rabie AB (2006). Effect of naringin on bone cells. *J Orthop Res* **24**: 2045–2050.

Wu JB, Fong YC, Tsai HY, Chen YF, Tsuzuki M, Tang CH (2008). Naringin-induced bone morphogenetic protein-2 expression via PI3K, Akt, c-Fos/c-Jun and AP-1 pathway in osteoblasts. *Eur J Pharmacol* **588**: 333–341.

Xie F, Wu CF, Lai WP, Yang XJ, Cheung PY, Yao XS *et al*. (2005). The osteoprotective effect of Herba epimedii (HEP) extract *in vivo* and *in vitro*. *Evid Based Complement Altern Med* **2**: 353–361.

Zhang Y, Leung PC, Che CT, Chow HK, Wu CF, Wong MS (2008). Improvement of bone properties and enhancement of mineralization by ethanol extract of Fructus *Ligustri Lucidi*. *Br J Nutr* **99**: 494–502.

Zhang Y, Dong XL, Lai WP, Helferich W, Wong MS (2009). Differential effects of genistein and a soy extract on three-dimensional bone parameters and the expression of bone specific genes in ovariectomized mice. *J Nutr* **139**: 2230–2236.